Vol 12 No 2, February 2003
1009-1963/2003/12(02)/0211-07

Chinese Physics

© 2003 Chin. Phys. Soc.
and IOP Publishing Ltd

Influence of isothermal approximation on the phase-field simulation of directional growth in undercooled melt*

Yu Yan-Mei(于艳梅)†, Yang Gen-Cang(杨根仓),
Zhao Da-Wen(赵达文), and Lü Yi-Li(吕衣礼)

State Key Laboratory of Solidification Processing, Northwestern Polytechnical University, Xi'an 710072, China

(Received 28 June 2002; revised manuscript received 14 October 2002)

By using the phase-field approach, we have simulated the directional growth of alloys in undercooled molten states under the isothermal and nonisothermal conditions. The influences of the isothermal approximation on simulation results are discussed. We found that for undercooling greater than 25K, the isothermal approximation overestimates the interface growth velocity and reduces a critical velocity for an absolute stable planar interface, thus in this simulation, the interface morphology shows the plane-cell-plane transition with increasing initial undercooling of the melt, and the planar interface obtained under a large undercooling is absolutely stable. Whereas in the nonisothermal simulation, only plane-cell transition occurs in the same range of the initial undercoolings of the melt, and the planar interface tends to be destabilized and evolve into cells.

Keywords: phase-field, isothermal approximation, directional growth, undercooling
PACC: 6150, 6470, 8140

1. Introduction

Alloy phase-field method is a useful approach for simulating the formation and evolution of all kinds of solid–liquid interfaces. Boettinger and Warren,[1] Conti,[2] and Kim and Kim[3] have simulated the cell to plane front transition during the directional solidification with a positive temperature gradient. In their simulations, the isothermal approximation is adopted, that is to say, the latent heat that is produced during solidifying is neglected, and the temperature field is treated approximately to be constant during solidification. In directional solidification, the isothermal approximation is considered to be reasonable because the imposed positive temperature gradient takes away the latent heat through the solid and, to a first approximation, does not affect the tip growth. However, in an undercooled melt, the latent heat is accumulated in the melt, causing a diffusive thermal field in the unsolidified undercooled melt, which renders the interface growth behaviour more complicated. Hence, the directional growth is controlled not only by the solute diffusion but also by the thermal diffusion. In this case, is the isothermal approximation still valid? In this paper, in order to evaluate the effect of isothermal approximation on the simulation results, the directional growth under different initial undercoolings is simulated using firstly the phase-field approach with the isothermal approximation (neglecting the latent heat), then the simulation is conducted again under the nonisothermal condition. In the nonisothermal simulation, the melt temperature is treated as a spatial and temporal variable, instead of being constant in the isothermal simulation.

2. Phase-field model and numerical technique

In this section, we derive the phase-field model, starting from a Landau–Ginzberg free energy function[4] which is written as

$$F = \int_V \left[f(\Phi, c, T) + \frac{1}{2}\varepsilon^2(\nabla\Phi)^2 + \frac{1}{2}\delta^2(\nabla c)^2 \right] \mathrm{d}V, \quad (1)$$

where f is the free energy density, Φ is the phase-field variable, c is the concentration of solute B in solvent A, T is the temperature, ε and δ are the coefficients

*Project supported by the National Natural Science Foundation of China (Grant No 59971037) and by the Northwestern Polytechnical University Doctoral Dissertation Innovation Foundation, China.

†Author to whom correspondence should be addressed. Tel.: +86-029-8493942-8022; Fax: +86-029-8491000
E-mail address: yanmeiyu@sina.com (Yu Yan-Mei).

which account for the gradient term corrections, and V is the region occupied by the system. Using this formulation, the phase-field model is obtained as follows

$$\frac{\partial \Phi}{\partial t} = M_\Phi \left[\nabla \varepsilon^2 \nabla \Phi - W g'(\Phi) - \frac{P'(\Phi)}{T}((1-c)f_A + c f_B) \right], \quad (2)$$

$$\frac{\partial c}{\partial t} = \nabla D_{\rm c} \left[\nabla c + \frac{v_{\rm m}}{RT} c(1-c) P'(\Phi)(f_A - f_B) \nabla \Phi \right], \quad (3)$$

$$\frac{\partial T}{\partial t} = K \nabla^2 T - \frac{(L_A(1-c) + cL_B)}{c_V} P'(\Phi) \frac{\partial \Phi}{\partial t} - \frac{(L_A - L_B)}{c_V}(1 - P(\Phi)) \frac{\partial c}{\partial t}, \quad (4)$$

where v_m is the molar volume, R is the ideal gas constant, f_A and f_B are the free energies of the pure elements A and B respectively. The solute diffusion coefficient $D_{\rm c}$ is supposed to be a function of Φ,

$$D_{\rm c} = D_{\rm s} + P(\Phi)(D_{\rm l} - D_{\rm s}), \quad (5)$$

where $D_{\rm s}$ and $D_{\rm l}$ are the solute diffusion coefficients in the solid and liquid, respectively.

For simplicity, we assume the same solid and liquid thermal diffusivities K and specific heat c_V for both states of the material, and omit the gradient correction in c.

M_Φ, W and ε are the phase-field parameters, related to the physical parameters: interfacial energy σ, atomic attach kinetic coefficient μ, meeting point $T_{\rm m}$, latent heat L, and interface thickness ξ, as shown in the following

$$M_\Phi = \frac{T_{\rm m}^2 \mu}{6\sqrt{2} L \xi}, \quad (6)$$

$$W = \frac{3\sigma}{\sqrt{2} T_{\rm m} \xi}, \quad (7)$$

$$\varepsilon^2 = \frac{6\sqrt{2}\sigma\xi}{T_{\rm m}}. \quad (8)$$

Choosing $M_\Phi(n) = M_\Phi$ and $\varepsilon(\boldsymbol{n}) = \varepsilon(1 + \gamma \cos(4\boldsymbol{n}))$ allows for anisotropies of the interfacial energy and interface kinetics, where $n = \dfrac{\nabla \Phi}{|\nabla \Phi|}$, γ is the magnitude of the anisotropy. The noise is included as proposed in Ref.[5], the amplitude of the fluctuations is taken to be 0.5.

Equations (2)–(4) are discretized in space using the second-order finite difference on uniform Cartesian grids, and in time using the first-order finite difference approximation. We use the ADI algorithm for the heat equation. To save the computation time, the computational domain is divided into two parts; in the inner region, which is of interest to the evolution of the phase and concentration fields, the grid spacing is selected to be $\Delta x = \xi$. With the grid spacing of 10–$50\Delta x$, the temperature field is resolved not only in the inner region, but also in the outer region where the changes of phase and concentration fields can be neglected. With the fixed size of the inner region, the outer region is extended continually to hold the far-field temperature at the initial value. The time step is specified in such a way that $\Delta t < \dfrac{\Delta x^2}{5D}$ according to $D = D_{\rm c}$ or $D = M_\Phi \varepsilon^2$ for keeping stable of the melt under time-step iterations. The zero Neumann boundary conditions for Φ, c and T are imposed at the boundaries of the computational domain.

In the subsequent simulations, the whole region is initially filled with uniformly undercooled melt. Assuming that the melt has solidified with a flat interface at one end of the computation region, the initial phase field and the concentration field are taken as step functions that represent a full equilibration of the liquid of concentration c_0 with the solid at a sharp interface. We choose the Ni–Cu alloys of different initial undercoolings for the simulations. The liquid and solid diffusion coefficients are taken to be 1.0×10^{-5} and 1.0×10^{-9} $\rm cm^2 \cdot s^{-1}$ respectively, and the thermal diffusion to be 0.115 $\rm cm^2 \cdot s^{-1}$. In fact, the solute and thermal diffusion is a variable depending on the local temperature and concentration, this leads to a variable mobility. In Ref.[6], a phase-field simulation with the mobility (diffusivity) depending on local compositions was conducted to study the coarsening kinetics of the interconnected two-phase mixtures, whereas in solidification constant diffusivities are usually adopted considering that the error brought by this approximate treatment does not influence the qualitative simulation results.[7,8] The heat capacity, latent heat of fusion, and surface energy are taken to be the realistic values.[5] But for saving the computational time, we take the interface thickness to be 5×10^{-6} cm, which is much larger than what is physically reasonable, and an interface attachment coefficient of $0.33 \rm cm \cdot s^{-1} K^{-1}$, which is 500 times smaller than that for collision-limited growth of the Ni–Cu alloy. This leads to the underestimation of the growth velocity. In spite of these limitations, we can obtain the qualitative and useful results of the simulations.[9]

3. Results and discussion

3.1. The interface morphology of Ni–Cu alloy

The interface morphologies obtained under the isothermal and nonisothermal conditions at the different initial undercoolings of the melt are shown in Figs.1 and 2 respectively.

Figure 1 shows that in the isothermal approximation, when the initial undercooling $\triangle T$ increases from 16.86 to 46.6K, the interface morphology shows a plane-cell-plane transition. However, Fig.2 shows that after the isothermal condition is relaxed, only the plane-cell transition occurs in the same range of the initial undercooling. When the initial undercooling is low, for example $\triangle T$=16.86K, the interfacial morphologies in the isothermal and nonisothermal simulations are somewhat similar. But when the initial undercooling is enhanced, the obtained interfacial morphologies in the two kinds of simulation are evidently distinct from each other. This indicates the important influence of the latent heat on the directional growth in the undercooled melt.

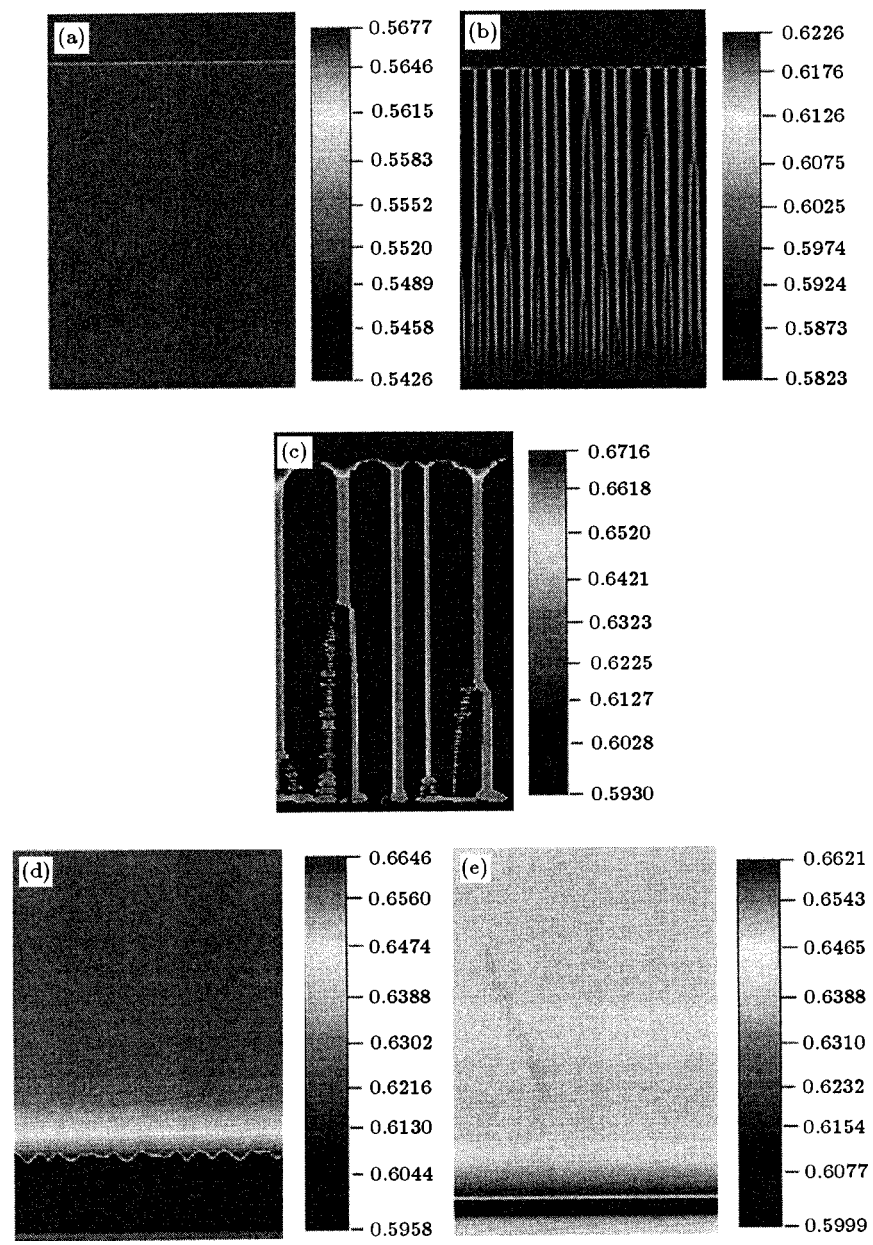


Fig.1. Interface morphologies of Cu-Ni alloys under different initial undercoolings obtained in the isothermal approximation. (a) $\triangle T$=46.6K; (b) $\triangle T$=30.0K; (c) $\triangle T$=26.75K; (d) $\triangle T$=23.46K; (e) $\triangle T$=16.86 K.

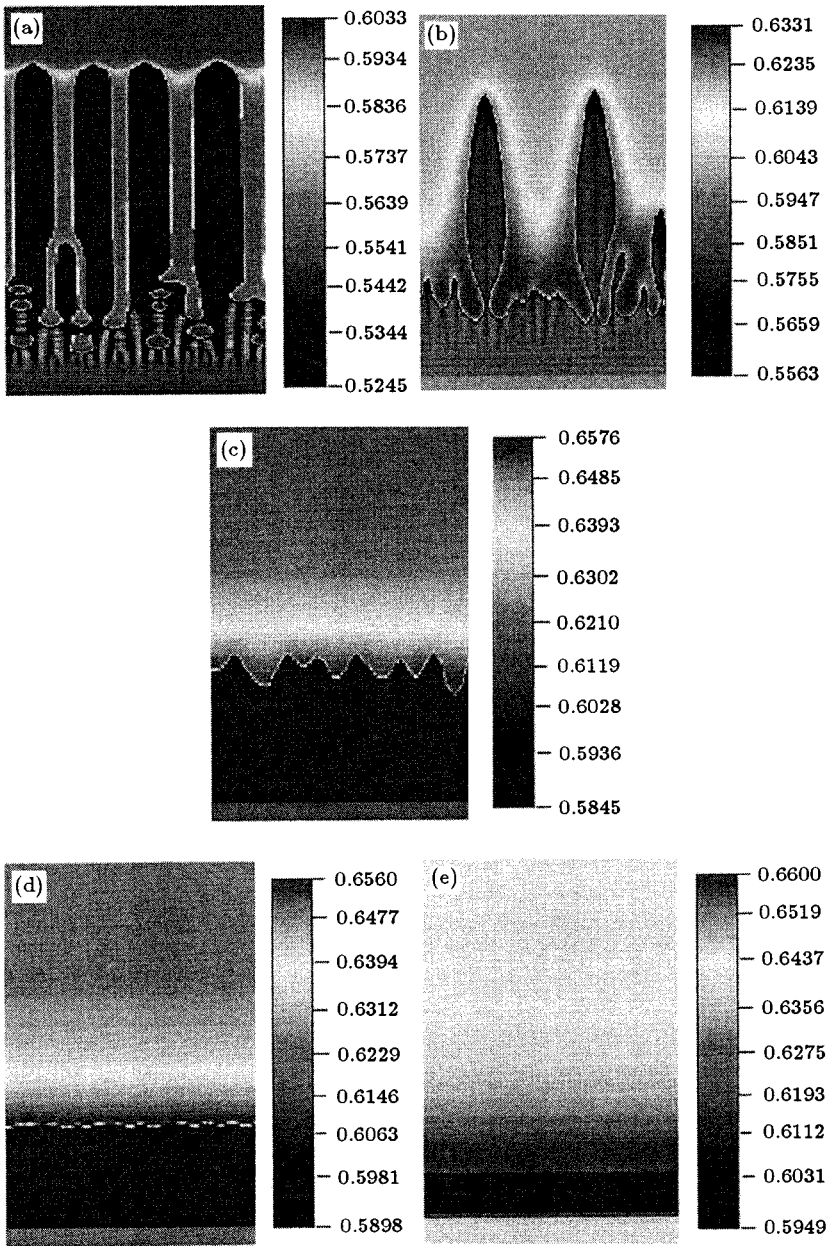


Fig.2. Interface morphologies of the Cu-Ni alloy at different initial undercoolings, obtained under the nonisothermal condition. (a) $\triangle T$=46.6K; (b) $\triangle T$=30.0K; (c) $\triangle T$=26.75K; (d) $\triangle T$=23.46 K; (e) $\triangle T$=16.86 K.

Usually, the interface stability exhibits the plane-cell-dendrite-cell-plane transition with the variation of the solidifying condition. We note that no dendrite is found in our simulation, which can be attributed to our simulation condition. In our simulation, in the direction along the principal axis of the cell, the computation region is continually extended so that the far-field melt in this direction remains at the initial condition quite well, and the heat and solute ejected during the cell growth have enough space to release. Therefore, the cell may develop fully in this direction However, the size of the computation regions in the lateral directions is fixed, and the lateral growing space of the cell is also limited. At the same time, the zero Neumann boundary condition (a kind of adiabatic condition) of the concentration and temperature fields in the lateral boundaries of the computation region also baffle the release of the ejected heat and solute during the cell growth in the lateral directions; this suppresses intensively the growth of the side-branch of the cell. In this case, the cell cannot develop fully in the lateral directions to evolve a dendritic pattern. Therefore, no dendrite can be seen in our simulations.

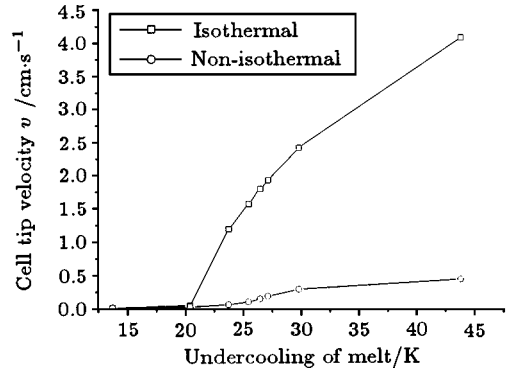


Fig.3. Cell tip velocities or pulling velocities of the plane fronts under different initial undercoolings of the melt.

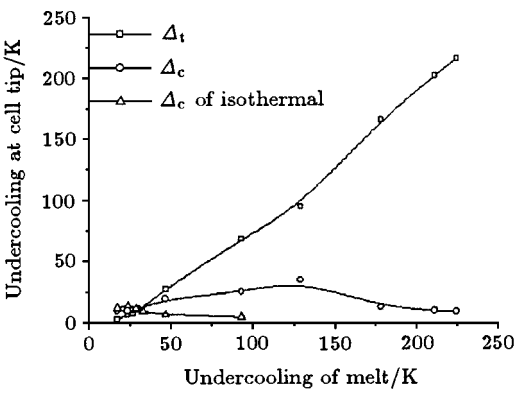


Fig.4. Undercoolings at the cell tips or the plane fronts under different initial undercoolings of the melt.

Figure 3 presents the cell tip velocities or pulling velocities of the plane fronts under different initial undercoolings of the melt in the isothermal and nonisothermal simulations. The isothermal velocities are consistent with the nonisothermal velocities when the melt undercoolings are less than about 20K, whereas for the melt undercoolings more than 20K, the tip velocities obtained by the isothermal simulation will greatly overrun those of the nonisothermal simulation. Figure 4 shows the undercoolings at the interface front in the melt at different initial undercoolings. Figure 4 also shows that there is a solute undercooling $\triangle T_{\rm c}$, but no thermal undercoolings $\triangle T_{\rm t}$ ahead of the interface under the isothermal condition, whereas there exist not only the solute undercooling but also the thermal undercooling under the nonisothermal condition. This means that under the isothermal condition the directional growth in an undercooled melt is controlled by the solute diffusion, whereas it is controlled by both of the solute and thermal diffusion under the nonisothermal condition. When the initial undercooling is less than 20K, $\triangle T_{\rm c}$ is the key factor that controls the directional growth. This makes no marked difference, whether $\triangle T_{\rm t}$ is considered or not. Therefore, when $\triangle T$=16.86K, the interfacial morphologies obtained by the isothermal and nonisothermal simulations are similar, as shown in Figs.1 (e) and 2 (e), and their corresponding tip velocities are consistent with each other. However, when the initial undercooling is greater than 20K, $\triangle T_{\rm t}$ increases continually and overruns $\triangle T_{\rm c}$ gradually with increasing initial undercooling of the melt. Thus, $\triangle T_{\rm t}$ becomes the dominant ingredient of the undercoolings ahead of the interface. We find that when the initial undercooling of the melt is larger than 20K, the diffusion of the latent heat will control the directional growth of the undercooled melt, here, the influence of the latent heat on growth has to be considered.

According to Boettinger–Coriell–Trivedi model,[10,11] we have

$$\triangle T = \triangle T_{\rm c} + \triangle T_{\rm t} + \triangle T_{\rm k} + \triangle T_{\rm r}, \qquad (9)$$

where $\triangle T$, $\triangle T_{\rm c}$, $\triangle T_{\rm t}$, $\triangle T_{\rm k}$ and $\triangle T_{\rm r}$ denote the initial undercooling of the melt, the solute undercooling, the thermal undercooling, the kinetic undercooling, and the curvature undercooling respectively.

The experimental research indicates that the curvature undercooling is usually very small, and its variation with the initial undercooling of the melt is slight, hence $\triangle T_{\rm r}$ can be neglected here. So, for the isothermal simulation we have $\triangle T = \triangle T_{\rm c} + \triangle T_{\rm k}$, and for the nonisothermal simulation $\triangle T = \triangle T_{\rm c} + \triangle T_{\rm t} + \triangle T_{\rm k}$. Figure 4 shows that when the initial undercooling of the melt is larger than 20K, $\triangle T_{\rm c}$ of the isothermal simulation is less than $\triangle T_{\rm t}$ and $\triangle T_{\rm c}$ of the nonisothermal simulation, hence for the same initial undercoolings, $\triangle T_{\rm k}$ in the isothermal simulation must be larger than that in the nonisothermal simulation. The kinetic undercooling is proportional to the growth velocity, hence in this situation, the growth velocity obtained by the isothermal simulation is necessarily larger than that by the nonisothermal simulation.

The above analysis indicates that for higher undercooling, due to neglecting the latent heat, the isothermal approximation overestimates the growth velocity. Therefore, in the same range of the initial undercoolings, the interface morphology shows the plane-cell-plane transition in the isothermal simulation, but the nonisothermal simulation only presents the plane-cell transition.

3.2. The plane interface stability in an undercooled melt

Figure 1 shows that for the low initial undercooling of 16.86K, the interfacial morphologies in isothermal and nonisothermal simulations are both planar. In the isothermal simulations, the interface morphology obtained becomes planar again when $\triangle T$=46.6K. When it lies between 16.86 and 46.6K, the interface has a cellular structure, and the variation of the corresponding cell tip radius against the initial undercoolings is given in Fig.5. As shown in Fig.5, when $\triangle T$ <26K, with increasing initial undercooling, the cell tip radius decreases, but in contrast when $\triangle T$ >26K, the cell tip radius increases with increasing initial undercoolings; and when $\triangle T$=46.6K, the interface obtained becomes planar again (here, the corresponding cell tip radius is infinite). Figure 5 also presents the variation of the cell tip radius against the initial undercooling in the nonisothermal simulations. When $\triangle T$ <26K, the variation of the cell tip radius against the initial undercooling is same as that in isothermal simulation. When $\triangle T$ >26K, the cell tip radius also increases with increasing initial undercoolings. However, the increase is slower than in the isothermal simulation; but when $\triangle T$=225K, the obtained interface also become a plane.

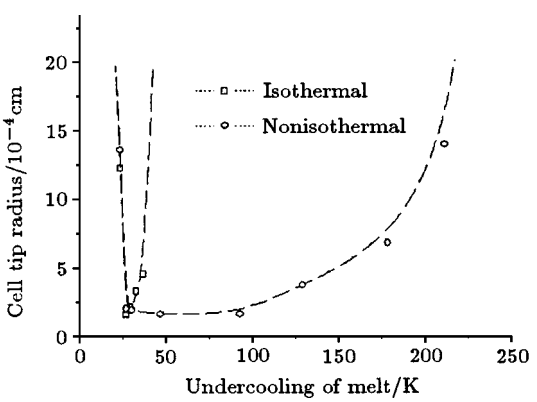


Fig.5. Cell tip radii against different initial undercoolings of the melt.

Both the isothermal simulation with $\triangle T$=46.6K and the nonisothermal simulation with $\triangle T$=225K acquire a planar interface at the same growth time. Figures 6 and 7 illustrate the variations of the perturbation wavelength ahead of, and the pulling velocity at the interface against time. Figure 6 presents a constant perturbation wavelength, a steady pulling velocity that produces a solute partition coefficient of 0.98, and a flimsy solute diffusion distance of 2.5×10^{-6} cm of the same magnitude as the perturbation wavelength. The solute capillarity length ($\sim \Gamma/\triangle T_0$, Γ is the Gibbs–Thomson coefficient, $\triangle T_0$ is the equilibrium solidification temperature range) is about 1.0×10^{-6} cm for $\Gamma=2.97\times10^{-5}$ cm·K and $\triangle T_0$=30K in this paper. The solute diffusion distance approaches the solute capillarity length, so an absolute stable planar interface is produced.[12] The constant disturbance wavelength and the steady pulling velocity shown in Fig.6 verify the absolute stability of the planar interface obtained when $\triangle T$=46.6K in the isothermal approximation.

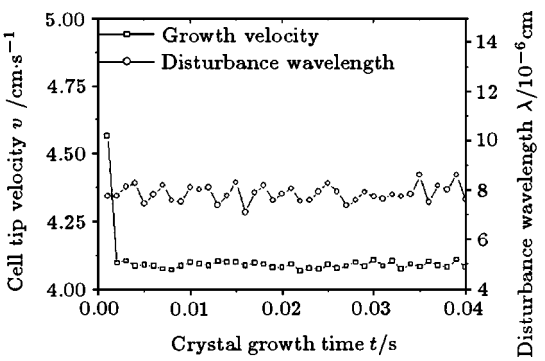


Fig.6. Interface pulling velocity and perturbation wavelength obtained when $\triangle T$=46.6K in the isothermal approximation.

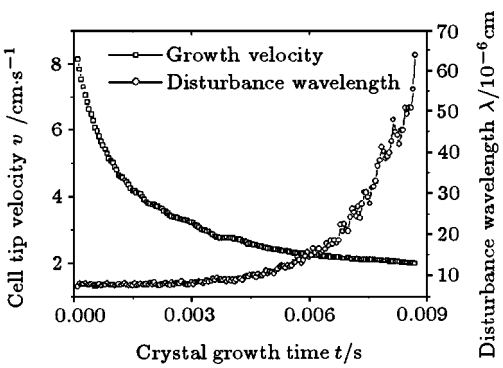


Fig.7. Interface pulling velocity and perturbation wavelength obtained when $\triangle T$=225K under the nonisothermal condition.

In contrast, under the nonisothermal condition, the perturbation wavelength begins suddenly to rise up rapidly after coming through the initial stable regime as shown in Fig.7. The increasing perturbation will break the planar interface only if the growth time is designed to be longer.

The critical velocity for the absolute stability in an undercooled melt, V_a, is given by $V_a = (V_a)_c+(V_a)_t$, the subscripts, c and t, indicate the limiting velocities that are controlled by the solute diffusion and thermal diffusion respectively. Due to neglecting the latent heat, $(V_a)_t$=0 in the isothermal simulation, so this approximation not only overestimates the growth velocity, but also reduces the critical growth rate for

the absolute stability. This is why the absolute stable planar interface can be readily achieved under the isothermal condition.

4. Conclusion

The isothermal and nonisothermal simulations of the directional growth in an undercooled melt present the different interfacial morphologies and the plane interface stability with increasing initial undercoolings of the melt. This indicates the important influences of the latent heat on the directional growth in the undercooled melt. When the initial undercooling is larger than 20K, the isothermal approximation with neglecting the latent heat leads to an overrating of the interface growth velocity; at the same time, it reduces the critical velocity of the absolute stable planar interface, therefore in the isothermal simulation with increasing initial undercoolings, the interfacial morphologies exhibit a plane-cell-plane transition, and at a high initial undercoolings of the melt, the absolute stable planar interface can be achieved. However, in the nonisothermal simulation, only the plane-cell transition occurs in the same range of the initial undercoolings, and the plane interface tends to destabilize and turns into cells.

References

[1] Boettinger W J and Warren J A 1999 *J. Crystal. Growth* **200** 583

[2] Conti M 1998 *Phys. Rev.* E **58** 6101

[3] Kim S G and Kim W T 2001 *Mater. Sci. Eng.* A **281** 304

[4] Langer J S 1986 *Directions in Condensed Matter Physics* eds Grinstein G and Mazenko G (Singapore: World Scientific Publ.)

[5] Warren J A and Boetinger W J 1995 *Acta. Metall. Mater.* **43** 689

[6] Jingzhi Z and Longqing C 1999 *Phys. Rev.* E **60** 3564

[7] Loginova L and Amberg G 2001 *Acta Mater.* **49** 573

[8] Conti M 1997 *Phys. Rev.* E **56** 3197

[9] Yu Y M, Yang G C, Zhao D W, Lü Y L, A Karma and C Beckermann 2001 *Acta Phys. Sin.* **50** 2423 (in Chinese)

[10] Boetinger W J, Coriell S R and Trivedi R 1988 *Rapid Solidification Processing: Principles and Technology* IV (Claitor's, Baton Rouge, LA) p13

[11] Chongru R *et al* 2001 *Acta Phys. Sin.* **50** 377 (in Chinese)

[12] Kurz W and Fisher D J 1984 *Fundamentals of Solidification* (Switzerland: Trans Tech Publ.)